Synthesis and Characterization of the Monomeric Phosphinogallanes $Bu^t_2GaPR'R''$ (R', R'' = bulky aryl or silyl groups) and Related Compounds†

Mark A. Petrie and Philip P. Power*
Department of Chemistry, University of California, Davis, California 95616, USA

The use of bulky substituent groups has allowed the isolation and spectroscopic and structural characterization of several monomeric phosphinogallanes wherein gallium and phosphorus are three-co-ordinate. These new compounds have the formula $Bu^t_2GaP(R)(SiPh_3)$ (R = $C_6H_2Bu^t_3$-2,4,6 **1**, $C_6H_2Pr^i_3$-2,4,6 **2**, $C_6H_2Me_3$-2,4,6 **3** or $SiMe_3$ **4**). Variable-temperature ^1H NMR studies indicate that there is a rotational barrier of *ca.* 12.7 kcal mol^{-1} around the Ga–P bond in **1** which has been attributed to weak Ga–P π bonding. The synthesis and structures of the related aluminium–phosphorus species $Bu^t_2Al(Et_2O)$-$P(C_6H_2Pr^i_3$-2,4,6)$(SiPh_3)$ **5** and the gallium–arsenic species $Bu^t_2GaAs[CH(SiMe_3)_2](SiPh_3)$ **6** are also reported. In addition, variable-temperature ^1H NMR studies of the precursor asymmetric phosphines $(Ph_3Si)P(R)H$ (R = $C_6H_2Bu^t_3$-2,4,6 **7**, $C_6H_2Pr^i_3$-2,4,6 **8** or $C_6H_2Me_3$-2,4,6 **9**) as well as the X-ray structures of $(Ph_3Si)P(C_6H_2Bu^t_3$-2,4,6)H **7** and $(Ph_3Si)P(SiMe_3)_2$ **10** are discussed. Crystal data with Mo-Kα radiation (λ = 0.710 69 Å) at 130 K: **2**, monoclinic, space group $P2_1/c$, a = 18.499(5), b = 10.028(4), c = 20.746(6) Å, β = 90.45(1)°, Z = 4, R = 0.043; **5**, triclinic, space group $P\bar{1}$, a = 9.488(3), b = 11.416(5), c = 20.383(6) Å, α = 92.07(3), β = 96.80(2), γ = 103.17(3)°, Z = 2, R = 0.079; **6**, triclinic, space group $P\bar{1}$, a = 12.219(3), b = 14.174(3), c = 21.831(5) Å, α = 92.95(2), β = 99.73(2), γ = 99.47(2)°, Z = 4, R = 0.053; **7**, monoclinic, space group $P2_1/c$, a = 17.710(6), b = 16.635(5), c = 10.838(4) Å, β = 97.43(3)°, Z = 4, R = 0.044; **10**, orthorhombic, space group $Pbca$, a = 16.092(5), b = 16.841(5), c = 18.778(5) Å, Z = 8 and R = 0.050.

There has been widespread interest in multiple bonding between the Main Group 13 and 15 elements for many years. Much of this work has been concerned with boron–nitrogen compounds and it is only very recently that π bonding between boron and the heavier Group 15 elements phosphorus and arsenic has become well established.[1–4] Likewise, information regarding π bonding in compounds where both of the Main Group 13 and 15 atoms are heavier members of their respective groups has been very sparse. Nonetheless, the recently reported structures of the Zintl anions $[M_2E_4]^{6-}$ (M = Al or Ga, E = P or As), which have planar M_2E_2 cores and short M–E bond lengths, support the presence of considerable M–E multiple interaction.[5] In addition, the synthesis and structural characterization of gallium–phosphorus species which are analogues of ethylene, $Bu^t_2GaP(C_6H_2Bu^t_3$-2,4,6)$(SiPh_3)$ or the allyl cation, $(C_6H_2Me_3$-2,4,6)$P[Ga(C_6H_2Pr^i_3$-2,4,6)$_2]_2$ were very recently communicated from this laboratory.[6,7] Their structures consist of almost planar $C_2GaP(C)Si$ and $CP(GaC_2)_2$ cores and relatively short Ga–P distances, 2.295(5) and 2.257(3) Å, respectively. Variable-temperature ^1H NMR studies of these gallium–phosphorus species indicated barriers to rotation around the Ga–P bonds of 12.7 and 10.6 kcal mol^{-1}, respectively. These barriers were attributed to weak Ga–P π interactions. It appears that one of the major factors in determining the extent of multiple bonding in these species and compounds of the general formulae $R_2ME(R')R''$ (where M = Ga or Al and E = P or As) is the inversion barrier at the phosphorus or arsenic centre. This normally ranges from *ca.* 0 to 36 kcal mol^{-1} for phosphanes and can be as high as 45 kcal mol^{-1} for arsanes.[8] It has been shown that, in certain boron–phosphorus and –arsenic compounds, large and electropositive substituents at phosphorus or arsenic lower the inversion barrier and induce stronger multiple bonding.[4,9] This paper reports similar investigations of Ga–P and Ga–As species. Several examples of new gallium–phosphorus compounds of the formulae $Bu^t_2GaP(R)(SiPh_3)$ (R = bulky aryl or silyl group) and related aluminium–phosphorus and gallium–arsenic species are reported here. In addition, variable-temperature ^1H NMR studies of the asymmetric phosphine precursors $(Ph_3Si)P(R)H$ are also presented.

Experimental

All experiments were performed either by using modified Schlenk techniques or in a Vacuum Atmospheres HE 43-2 dry box under nitrogen. Solvents were freshly distilled from a sodium–potassium alloy and degassed twice prior to use. Phosphorus-31 and ^1H NMR spectra were recorded in C_6D_6 or C_7D_8 solutions using a General Electric QE-300 spectrometer. The compounds $GaBu^t_2Cl$,[10] $AlBu^t_2Cl$,[11] $PH_2(C_6H_2Bu^t_3$-2,4,6),[12] $PH_2(C_6H_2Pr^i_3$-2,4,6),[13] $PH_2(C_6H_2Me_3$-2,4,6),[14] $(Me_3Si)_2PLi$·2thf[15] (thf = tetrahydrofuran) and $(Me_3Si)_2$-$CHAsH_2$[16] were synthesized according to literature methods. Chlorotriphenylsilane was purchased commercially and used as received.

Preparations.—$Bu^t_2GaP(R)(SiPh_3)$ (R = $C_6H_2Bu^t_3$-2,4,6 **1**, $C_6H_2Pr^i_3$-2,4,6 **2** *or* $C_6H_2Me_3$-2,4,6 **3**). The compounds **1–3** were prepared in an identical manner. The synthesis of **1** is described here. An Et_2O (20 cm^3) solution of $(Ph_3Si)P(C_6H_2$-Bu^t_3-2,4,6)H (2.15 g, 4 mmol) **7** (synthesis described below) was treated dropwise with $LiBu^n$ (2.5 cm^3 of a 1.6 mol dm^{-3} hexane solution, 4 mmol). After stirring for 3 h at room temperature $GaBu^t_2Cl$ (0.86, 4 mmol) in Et_2O (15 cm^3) was added dropwise and the solution was stirred for a further 4 h. The volatile materials were removed under reduced pressure and the residue was taken up in pentane (30 cm^3). Filtration and concentration

† *Supplementary data available:* see Instructions for Authors, *J. Chem. Soc., Dalton Trans.*, 1993, Issue 1, pp. xxiii–xxviii.
Non-SI unit employed: cal ≈ 4.184 J.

Table 1 Microanalytical data for compounds **2**–**11** *

Compound	C	H
2 $Bu^t_2GaP(C_6H_2Pr^i_3$-2,4,6)$(SiPh_3)$	72.90 (72.65)	8.40 (8.35)
3 $Bu^t_2GaP(C_6H_2Me_3$-2,4,6)$(SiPh_3)$	71.00 (70.80)	7.50 (7.45)
4 $Bu^t_2GaP(SiMe_3)(SiPh_3)$	62.70 (62.50)	9.45 (9.40)
5 $Bu^t_2Al(Et_2O)P(C_6H_2Pr^i_3$-2,4,6)$(SiPh_3)$	76.10 (76.20)	9.40 (9.40)
6 $Bu^t_2GaAs[CH(SiMe_3)_2](SiPh_3)$	58.45 (58.50)	7.80 (7.75)
7 $(Ph_3Si)P(C_6H_2Bu^t_3$-2,4,6)H	79.10 (78.95)	8.35 (8.30)
8 $(Ph_3Si)P(C_6H_2Pr^i_3$-2,4,6)H	80.60 (80.10)	8.00 (7.95)
9 $(Ph_3Si)P(C_6H_2Me_3$-2,4,6)H	80.40 (79.00)	6.95 (6.65)
10 $(Ph_3Si)P(SiMe_3)_2$	66.35 (66.00)	7.65 (7.60)
11 $(SiMe_3)(SiPh_3)PLi$·dme	65.85 (65.20)	7.80 (7.45)

* Required values are given in parentheses.

to *ca.* 10 cm^3 and cooling to −78 °C gave a white solid which may be recrystallized from a minimum volume of hexane or Et_2O in a freezer at −20 °C. $Bu^t_2GaP(C_6H_2Bu^t_3$-2,4,6)$(SiPh_3)$ **1**: yield 2.07 g, 72%; m.p. 154–158 °C. NMR: ^1H (C_7D_8, 25 °C), δ 1.12 (s, 18 H, $GaBu^t_2$), 1.58 (s, 18 H, *o*-Bu^t), 1.3 (s, 9 H, *p*-Bu^t), 7.05 (m, 8 H, *m*-H of $C_6H_2Bu^t_3$-2,4,6 and $SiPh_3$) and 7.65 (mm, 9 H, *o*- and *p*-H of $SiPh_3$); ^{31}P (C_6D_6), δ −119. $Bu^t_2GaP(C_6H_2Pr^i_3$-2,4,6)$(SiPh_3)$ **2**: yield 68%; m.p. 138–143 °C. NMR: ^1H (C_7D_8), δ 1.02 [d, 12 H, *o*-$CH(CH_3)_2$], 1.03 (s, 18 H, $GaBu^t_2$), 1.19 [d, 6 H, *p*-$CH(CH_3)_2$], 2.77 [spt, 1 H, *p*-$CH(CH_3)_2$], 4.39 [spt, 2 H, *o*-$CH(CH_3)_2$], 7.12 (m, 8 H, *m*-H of $C_6H_2Pr^i_3$-2,4,6 and $SiPh_3$) and 7.65 (mm, 9 H, *o*- and *p*-H of $SiPh_3$); ^{31}P (C_6D_6), δ −146. $Bu^t_2GaP(C_6H_2Me_3$-2,4,6)$(SiPh_3)$ **3**: yield 52%; m.p. 74–79 °C. NMR (C_7D_8): ^1H, δ 1.03 (s, 18 H, $GaBu^t_2$), 2.04 (s, 3 H, *p*-Me), 2.37 (s, 3 H, *o*-Me), 7.12 (m, 8 H, *m*-H of $C_6H_2Me_3$-2,4,6 and $SiPh_3$) and 7.70 (m, 9 H, *o*- and *p*-H of $SiPh_3$); ^{31}P, δ −141.

$Bu^t_2GaP(SiMe_3)(SiPh_3)$ **4**. A dimethoxyethane (dme) solution (20 cm^3) of $(Ph_3Si)P(SiMe_3)_2$ **10** (1.62 g, 3.7 mmol) at −10 °C was treated dropwise with a 1.5 mol dm^{-3} Et_2O solution of LiMe (2.47 cm^3, 3.7 mmol). After stirring for 3 h at −10 °C the solution was allowed to warm and stirred for another 12 h. The volatile materials were removed under reduced pressure and the residue was dissolved in Et_2O (20 cm^3). The Et_2O solution of **11** was added *via* cannula to $GaBu^t_2Cl$ (0.81 g, 3.7 mmol) in Et_2O (20 cm^3) at 0 °C. After warming to room temperature and stirring for 5 h, the Et_2O was removed and replaced with pentane (50 cm^3, the product decomposes if heated). Filtration, and concentration to *ca.* 15 cm^3 then cooling to −20 °C for 2 d gave **4** as colourless prisms. Yield: 1.42 g, 70%; m.p. 111–118 °C (decomp. to yellow oil). NMR: ^1H (C_7D_8), δ 0.194 (d, 9 H, $SiMe_3$, $^3J_{P-H}$ 5.7 Hz), 1.10 (s, 18 H, $GaBu^t_2$), 7.14 (m, 6 H, *m*-H of $SiPh_3$) and 7.80 (m, 9 H, *o*- and *p*-H of $SiPh_3$); ^{31}P (C_6D_6), δ −267.

$Bu^t_2Al(Et_2O)P(C_6H_2Pr^i_3$-2,4,6)$(SiPh_3)$ **5**. To a solution of **8** (1.48 g, 3 mmol) in pentane (30 cm^3), was rapidly added $LiBu^n$ (1.88 cm^3, 1.6 mol dm^{-3} in hexanes). No reaction was observed until ≈5 cm^3 of Et_2O was added to the solution. After stirring for 3 h, all volatiles were removed and the solid rinsed twice with two portions of pentane (30 cm^3). A pentane solution (20 cm^3) of $AlBu^t_2Cl$ (0.53 g, 3 mmol) was added to a pentane (30 cm^3) slurry of the resulting solid and the solution was stirred for a further 3 h. Filtration and concentration to *ca.* 3 cm^3 and cooling in a freezer at −20 °C afforded a crystalline product; yield 0.91 g, 43%; m.p. 109–112 °C. NMR: ^1H (C_7D_8), δ 0.781 (m, 6 H, Et_2O), 1.06 (s, 18 H, $AlBu^t_2$), 1.10 [d, 12 H, *o*-$CH(CH_3)_2$], 1.25 [d, 6 H, *p*-$CH(CH_3)_2$], 2.80 [spt, 1 H, *p*-$CH(CH_3)_2$], 3.63 (m, 4 H, Et_2O), 4.78 [spt, 2 H, *o*-$CH(CH_3)_2$], 7.08 (m, 8 H, *m*-H of $C_6H_2Pr^i_3$-2,4,6 and $SiPh_3$) and 7.62 (m, 9 H, *o*- and *p*-H of $SiPh_3$); $^{31}P(C_6D_6)$, δ −199.

$Bu^t_2GaAs[CH(SiMe_3)_2](SiPh_3)$ **6**. In a typical preparation of the asymmetric arsine the primary arsine $(Me_3Si)_2CHAsH_2$ (2.36 g, 10 mmol) was slowly treated dropwise with $LiBu^n$ (6.25 cm^3 of 1.6 mol dm^{-3} solution in hexanes, 10 mmol) in Et_2O (40 cm^3) at −78 °C. After warming to room temperature and stirring for 30 min an Et_2O (20 cm^3) solution of Ph_3SiCl (2.95 g, 10 mmol) was added dropwise at 0 °C. After stirring for ≈12 h all volatile materials were removed and the residue extracted with pentane (40 cm^3) and filtered over Celite. Colourless crystals of the product separated from solution after cooling to −20 °C in an almost quantitative yield. The species **6** was prepared from the secondary arsine $Ph_3SiAs[CH(SiMe_3)_2]H$ in an identical manner to **1**–**3** in ≈55% yield, m.p. >115 °C (decomp. to yellow oil). ^1H NMR (C_6D_6), δ 0.07 [s, 18 H, $CH(SiMe_3)_2$], 1.07 (s, 18 H, $GaBu^t_2$), 1.85 [s, 1 H, $CH(SiMe_3)_2$], 7.08 (m, 6 H, *m*-H of $SiPh_3$) and 7.85 (9 H, *o*- and *p*-H of $SiPh_3$).

$(Ph_3Si)P(R)H$ (R = $C_6H_2Bu^t_3$-2,4,6 **7**, $C_6H_2Pr^i_3$-2,4,6 **8** or $C_6H_2Me_3$-2,4,6 **9**). The asymmetrically substituted phosphines were prepared in an analogous manner. The synthesis of **7** is described here. To an Et_2O (50 cm^3) solution of $LiPH(C_6H_2Bu^t_3$-2,4,6) (10 mmol) prepared *in situ* from $PH_2(C_6H_2Bu^t_3$-2,4,6) (2.78 g, 10 mmol) and $LiBu^n$ (6.25 cm^3, 10 mmol) was added Ph_3SiCl (2.95 g, 10 mmol) in Et_2O (30 cm^3) dropwise. The cloudy solution was allowed to stir for 12 h. All volatile materials were removed under reduced pressure and the residue was taken up in pentane (40 cm^3). After filtration the solution was pumped down to incipient crystallization. Slow cooling in a freezer at −20 °C overnight afforded the product in ≈90% yield. $(Ph_3Si)P(C_6H_2Bu^t_3$-2,4,6)H **7**: m.p. 153–156 °C. NMR (C_6D_6): ^1H, δ 1.36 (s, 9 H, *p*-Bu^t), 1.43 (d, 18 H, *o*-Bu^t), 5.19 (d, 1 H, P–H), 7.09 (m, 8 H, *m*-H of $C_6H_2Bu^t_3$-2,4,6 and $SiPh_3$), 7.44 (m, 9 H, *o*- and *p*-H of $SiPh_3$); ^{31}P, δ −132 (J_{P-H} 220 Hz). $(Ph_3Si)P(C_6H_2Pr^i_3$-2,4,6)H **8**: m.p. 120–127 °C. NMR (C_6D_6): ^1H, δ 0.98 [d, 6 H, *o*- or *p*-$CH(CH_3)_2$], 1.09 [d, 6 H, *o*- or *p*-$CH(CH_3)_2$], 1.29 [d, 6 H, *o*- or *p*-$CH(CH_3)_2$], 2.83 [spt, 1 H, *p*-$CH(CH_3)_2$], 3.52 [spt, 2 H, *o*-$CH(CH_3)_2$], 4.44 (d, 1 H, P–H), 7.18 (m, 8 H, *m*-H of $C_6H_2Pr^i_3$-2,4,6 and $SiPh_3$) and 7.60 (m, 9 H, *o*- and *p*-H of $SiPh_3$); ^{31}P, δ −169 (J_{P-H} 211 Hz). $(Ph_3Si)P(C_6H_2Me_3$-2,4,6)H **9**: m.p. 92–96 °C. NMR (C_6D_6): ^1H, δ 2.1 (s, 6 H, *o*-Me), 2.14 (s, 3 H, *p*-CH_3), 4.21 (d, 1 H, P–H), 7.2 (m, 8 H, *m*-H of $C_6H_2Me_3$-2,4,6 and $SiPh_3$), 7.61 (9 H, *o*- and *p*-H of $SiPh_3$); ^{31}P, δ −162, (J_{P-H} 210 Hz).

$(Ph_3Si)P(SiMe_3)_2$ **10**. An Et_2O (20 cm^3) solution of Ph_3SiCl (2.65 g, 9 mmol) was added dropwise at 0 °C to $(Me_3Si)_2PLi$·2thf (2.96 g, 9 mmol) in Et_2O (30 cm^3). The solution was allowed to stir for 12 h. After removing all volatile materials, the residue was extracted with warm hexane (40 cm^3) and filtered through Celite. Colourless crystals of the product separated from solution after cooling to −20 °C. Yield: 3.38 g, 86%; m.p. 97–99 °C. NMR (C_6D_6): ^1H, δ 0.254 (d, 18 H, $SiMe_3$, $^3J_{P-H}$ 3.9 Hz), 7.10 (m, 6 H, Ph) and 7.88 (m, 9 H, Ph); ^{31}P, δ −254.

$(Me_3Si)(Ph_3Si)PLi$·dme **11**. The detailed *in situ* preparation of **11** has been described earlier as part of the synthesis of **4**. Recrystallization of the dme solvated **11** is possible from Et_2O–hexane (2:1) in ≈80% yield. NMR (C_7D_8): ^1H, δ 0.274 (d, 9 H, $SiMe_3$), 2.97 (s, 6 H, OMe), 3.04 (s, 4 H, OCH_2), 7.21 (m, 6 H, Ph) and 7.98 (m, 9 H, Ph); ^{31}P, δ −315.

Analytical data for the new complexes are given in Table 1.

X-Ray Data Collection and the Solution and Refinement of the Structures.—Crystallographic data for compounds **2**, **5**–**7** and **10** are given in Table 2. Crystals of **2**, **5**–**7** and **10** were coated with a layer of hydrocarbon oil upon removal from the Schlenk tube. A suitable crystal was selected, attached to a glass fibre by silicon grease and immediately placed in the low-temperature N_2 stream.[17] X-ray data were collected with Siemens R3 m/V and Syntex $P2_1$ diffractometers equipped with a graphite monochromator and a locally modified Enraf-Nonius low-temperature apparatus. Calculations were carried out on a Microvax 3200 computer using the SHELXTL PLUS program system.[18] Neutral atom scattering factors and the correction for anomalous dispersion were from ref. 19. The structures of all molecules were solved by direct methods. Atomic coordinates

Table 2 Selected crystallographic data and structural parameters for compounds **2**, **5**–**7** and **10***

Compound	**2**	**5**	**6**	**7**	**10**
Formula	$C_{41}H_{56}GaPSi$	$C_{45}H_{66}AlOPSi$	$C_{33}H_{52}AsGaSi_3$	$C_{36}H_{45}PSi$	$C_{24}H_{33}PSi_3$
M_r	677.6	709	677.7	547.5	436.7
Crystal system	Monoclinic	Triclinic	Triclinic	Monoclinic	Orthorhombic
Space group	P_1/c	$P\bar{1}$	$P\bar{1}$	$P2_1/c$	*Pbca*
a/Å	18.499(5)	9.488(3)	12.219(3)	17.710(6)	16.092(5)
b/Å	10.028(4)	11.416(5)	14.174(3)	16.635(5)	16.841(5)
c/Å	20.746(6)	20.383(6)	21.831(5)	10.838(4)	18.778(5)
α/°	90	92.07(3)	92.95(2)	90	90
β/°	90.45(2)	96.80(2)	99.73(2)	97.43(3)	90
γ/°	90	103.17(3)	99.47(2)	90	90
U/Å	3848(2)	2127.2(16)	3663.7(15)	3166(2)	5089(3)
Z	4	2	4	4	8
D_c/g cm^{-3}	1.170	1.107	1.229	1.126	1.140
μ/mm^{-1}	0.813	0.145	1.765	0.147	0.257
2θ range/°	0–55	0–50	0–55	0–55	0–55
Number of observed reflections	5307 [$I > 3\sigma(I)$]	3921 [$I > 2\sigma(I)$]	11 957 [$I > 2\sigma(I)$]	5745 [$I > 2\sigma(I)$]	2843 [$I > 2\sigma(I)$]
Number of variables	398	442	614	347	253
R, R'	0.043, 0.045	0.079, 0.086	0.053, 0.104	0.044, 0.043	0.050, 0.052

* All data were collected at 130 K with Mo-Kα radiation (λ = 0.710 69 Å).

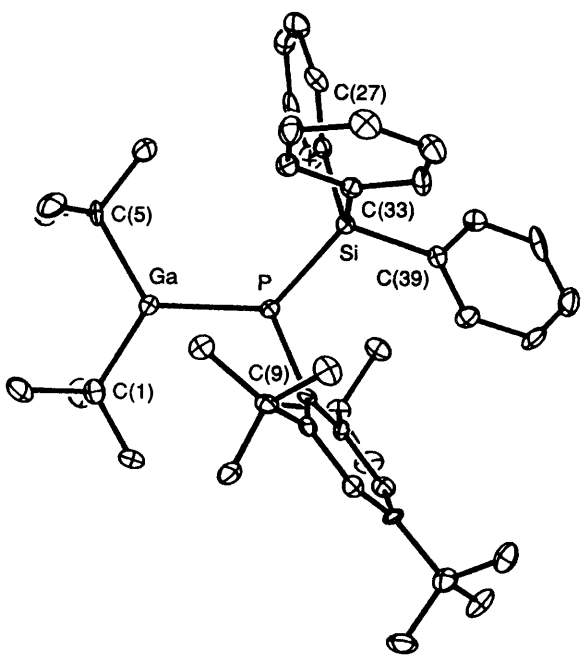

Fig. 1 Computer-generated thermal ellipsoid (30%) plot of compound **1**. Hydrogen atoms are omitted for clarity

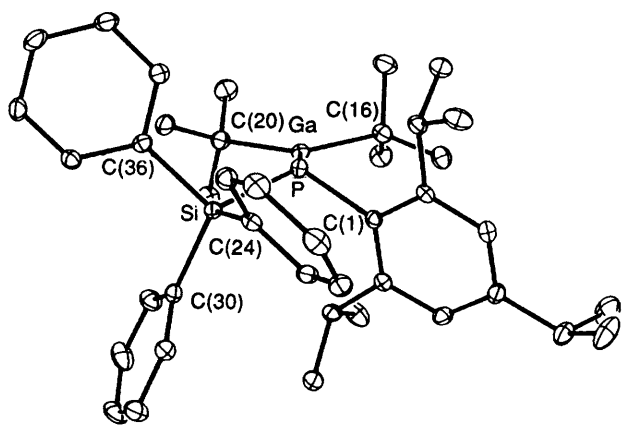

Fig. 2 Computer-generated thermal ellipsoid (30%) plot of compound **2**. Hydrogen atoms are omitted for clarity

for **2**, **5**–**7** and **10** are given in Table 3. An X-ray data set was also collected for **4**, however, severe disorder problems were encountered. Nonetheless, the data could be refined sufficiently to show that the Ga–P distance was 2.358(4) Å, and Σ°P was *ca.* 326°. Furthermore, a value of *ca.* 76.5° was calculated for the angle between the perpendiculars to the GaC_2 and PSi_2 planes.

Additional material available from the Cambridge Crystallographic Data Centre comprises H-atom coordinates, thermal parameters and remaining bond lengths and angles.

Results

Structural Descriptions.—The structure of compound **1**, shown in Fig. 1, was previously reported in a preliminary communication.[6] The structural descriptions of **7** and **10** are considered together here owing to the similarity of their formulae whereas **2** is considered separately. The structures of **5** and **6** are also described. Selected structural parameters for **1**, **2** and Bu^t_2 GaP(Ph)B($C_6H_2Me_3$-2,4,6) **12**[20] are summarized in Table 4. Important structural parameters for **5**–**7** and **10** are represented in Table 5.

$Bu^t_2GaP(C_6H_4Pr^i_3$-2,4,6)$(SiPh_3)$ **2**. The structure of **2**, which is illustrated in Fig. 2, consists of well separated monomers. The co-ordination at the phosphorus centre is pyramidal and the sum of the interligand angles (Σ°P) at phosphorus is 340.5°. The angle between the bisectors of the C_2Ga and CSiP planes is 1.9°. The Ga–P bond length is 2.296(1) Å and the P–Si and Ga–C distances are 2.249(2) and 2.012 Å (av.). The co-ordination geometry at gallium is trigonal planar.

$Bu^t_2Al(Et_2O)P(C_6H_2Pr^i_3$-2,4,6)$(SiPh_3)$ **5**. The molecular structure of **5**, which is represented in Fig. 3, contains phosphorus and aluminium centres with co-ordination numbers of three and four, respectively. The aluminium has distorted tetrahedral geometry with ligands that include $P(C_6H_2Pr^i_3$-2,4,6)$(SiPh_3)$, two *tert*-butyl groups and an Et_2O solvent molecule. The interligand angles at aluminium span the range 101.0(2) to 116.3(3)°, however, the sum of the angles between the two *tert*-butyl and phosphido groups is 341.7°. The sum of the angles at phosphorus (Σ°P = 351.6°) indicate a very flattened co-ordination. The Al–P bond length is 2.416(3) Å. The Al–O and Al–C distances are 1.950(6) and 2.021 Å (av.), respectively and the P–C(1) and P–Si bond lengths are 1.856(6) and 2.223(3) Å.

$Bu^t_2GaAs[CH(SiMe_3)_2](SiPh_3)$ **6**. There are two structurally similar monomeric gallium–arsenic molecules per asymmetric

Table 3 Atomic coordinates ($\times 10^4$) for compounds **2**, **5**–**7** and **10**

Atom	*x*	*y*	*z*	Atom	*x*	*y*	*z*
Compound **2**							
Ga	8 211(1)	9 883(1)	1 930(1)	C(20)	7 745(2)	8 546(3)	2 515(2)
P	7 660(1)	10 408(1)	967(1)	C(21)	7 165(2)	7 756(4)	2 154(2)
Si	6 484(1)	10 270(1)	693(1)	C(22)	8 298(2)	7 543(4)	2 798(2)
C(1)	7 915(2)	12 142(3)	774(2)	C(23)	7 405(2)	9 326(4)	3 071(2)
C(2)	8 285(2)	12 372(3)	190(2)	C(24)	6 435(2)	11 061(3)	−130(2)
C(3)	8 526(2)	13 660(3)	51(2)	C(25)	6 276(2)	10 299(4)	−676(2)
C(4)	8 403(2)	14 734(3)	459(2)	C(26)	6 231(2)	10 864(4)	−1 288(2)
C(5)	8 011(2)	14 491(3)	1 013(2)	C(27)	6 351(2)	12 225(4)	−1 365(2)
C(6)	7 759(2)	13 233(3)	1 178(2)	C(28)	6 511(2)	13 004(4)	−829(2)
C(7)	8 432(2)	11 253(3)	−292(2)	C(29)	6 551(2)	12 435(3)	−220(2)
C(8)	9 130(2)	10 525(4)	−129(2)	C(30)	5 787(2)	11 092(3)	1 218(2)
C(9)	8 447(2)	11 723(4)	−991(2)	C(31)	5 739(2)	10 819(4)	1 881(2)
C(10)	8 681(2)	16 132(4)	329(2)	C(32)	5 212(2)	11 399(5)	2 257(2)
C(11)	8 684(3)	16 502(4)	−384(2)	C(33)	4 726(2)	12 303(4)	1 989(2)
C(12)	9 421(2)	16 312(5)	638(2)	C(34)	4 758(2)	12 577(4)	1 340(2)
C(13)	7 317(2)	13 116(3)	1 798(2)	C(35)	5 276(2)	11 982(3)	957(2)
C(14)	6 664(2)	14 044(3)	1 788(2)	C(36)	6 265(2)	8 450(3)	608(2)
C(15)	7 788(2)	13 389(5)	2 395(2)	C(37)	6 738(2)	7 591(3)	290(2)
C(16)	9 245(2)	10 473(4)	2 053(2)	C(38)	6 561(2)	6 268(3)	176(2)
C(17)	9 695(2)	9 277(4)	1 830(2)	C(39)	5 902(2)	5 777(3)	376(2)
C(18)	9 410(2)	10 719(4)	2 769(2)	C(40)	5 430(2)	6 593(3)	704(2)
C(19)	9 471(2)	11 702(4)	1 676(2)	C(41)	5 607(2)	7 917(3)	812(2)
Compound **5**							
P	2 087(2)	8 050(2)	2 584(1)	C(22)	4 370(6)	11 039(6)	2 781(3)
Si	2 453(2)	10 046(2)	2 674(1)	C(23)	4 855(7)	11 857(6)	2 317(3)
Al	2 351(2)	6 739(2)	3 471(1)	C(24)	6 276(7)	12 571(7)	2 396(3)
O	2 936(5)	5 436(4)	3 011(2)	C(25)	7 226(7)	12 504(7)	2 952(4)
C(1)	2 622(6)	7 694(6)	1 767(3)	C(26)	6 762(7)	11 747(7)	3 431(4)
C(2)	1 517(6)	7 172(6)	1 236(3)	C(27)	5 370(6)	11 012(6)	3 353(3)
C(3)	1 857(6)	7 030(6)	610(3)	C(28)	1 512(6)	10 381(6)	3 389(3)
C(4)	3 283(6)	7 369(6)	457(3)	C(29)	2 112(7)	11 319(7)	3 883(3)
C(5)	4 383(6)	7 821(6)	984(3)	C(30)	1 346(9)	11 588(9)	4 380(4)
C(6)	4 083(6)	7 980(6)	1 622(3)	C(31)	−76(9)	10 935(9)	4 411(4)
C(7)	−112(6)	6 772(6)	1 337(3)	C(32)	−694(8)	9 988(8)	3 927(4)
C(8)	−776(7)	5 462(7)	1 079(4)	C(33)	77(7)	9 735(7)	3 436(3)
C(9)	−995(7)	7 594(7)	1 002(4)	C(34)	3 878(6)	7 430(6)	4 247(3)
C(10)	3 621(7)	7 278(6)	−253(3)	C(35)	5 422(7)	7 920(7)	4 063(3)
C(11)	4 600(9)	6 424(9)	−343(4)	C(36)	3 396(7)	8 523(7)	4 527(3)
C(12)	4 283(8)	8 501(7)	−484(3)	C(37)	4 022(8)	6 595(7)	4 813(3)
C(13)	5 388(6)	8 433(6)	2 167(3)	C(38)	346(7)	5 932(6)	3 691(3)
C(14)	6 060(7)	7 380(7)	2 377(3)	C(39)	−132(8)	6 673(8)	4 223(3)
C(15)	6 568(6)	9 440(6)	1 960(3)	C(40)	308(8)	4 697(7)	3 967(3)
C(16)	1 501(6)	10 549(6)	1 906(3)	C(41)	−865(7)	5 767(7)	3 089(3)
C(17)	1 911(7)	10 391(6)	1 273(3)	C(42)	3 470(11)	4 396(13)	3 428(5)
C(18)	1 213(7)	10 805(7)	724(3)	C(43)	4 910(13)	4 640(12)	3 374(5)
C(19)	87(8)	11 357(8)	785(3)	C(44)	2 062(8)	4 868(7)	2 386(3)
C(20)	−337(7)	11 536(7)	1 398(4)	C(45)	2 916(8)	4 525(8)	1 875(3)
C(21)	367(6)	11 135(6)	1 955(3)				
Compound **6**							
As(1)	2 018(1)	7 058(1)	1 302(1)	As(2)	8 370(1)	3 147(1)	3 796(1)
Ga(1)	444(1)	7 796(1)	1 551(1)	Ga(2)	6 502(1)	2 724(1)	3 122(1)
Si(1)	2 134(1)	7 583(1)	298(1)	Si(4)	7 949(1)	2 375(1)	4 683(1)
Si(2)	4 742(1)	7 523(1)	1 824(1)	Si(5)	9 463(2)	3 098(1)	2 584(1)
Si(3)	2 983(1)	7 247(1)	2 739(1)	Si(6)	10 775(1)	2 382(1)	3 813(1)
C(4)	4 559	5 913	−616	C(35)	5 624(3)	2 494(2)	4 634(1)
C(5)	4 670	6 906	−635	C(36)	4 716	2 884	4 783
C(6)	3 957	7 403	−361	C(37)	4 910	3 718	5 183
C(1)	3 133	6 907	−69	C(38)	6 012	4 162	5 434
C(8)	3 048(3)	9 587(2)	657(1)	C(39)	6 920	3 773	5 285
C(9)	3 372	10 538	532	C(34)	6 726	2 939	4 886
C(10)	3 193	10 796	−81	C(41)	6 773(3)	600(2)	4 991(2)
C(11)	2 690	10 103	−568	C(42)	6 392	−390	4 921
C(12)	2 367	9 152	−443	C(43)	6 715	−955	4 465
C(7)	2 546	8 894	170	C(44)	7 420	−532	4 078
C(14)	250(2)	6 234(2)	−404(2)	C(45)	7 802	458	4 147
C(15)	−850	5 955	−733	C(40)	7 479	1 024	4 603
C(16)	−1 569	6 626	−816	C(47)	9 590(3)	2 028(2)	5 722(2)
C(17)	−1 188	7 574	−571	C(48)	10 535	2 288	6 193
C(18)	−89	7 852	−242	C(49)	11 095	3 238	6 291
C(13)	630	7 182	−159	C(50)	10 710	3 928	5 918

Table 3 (*continued*)

Atom	*x*	*y*	*z*	Atom	*x*	*y*	*z*
C(19)	3 321(3)	7 694(3)	1 972(2)	C(51)	9 765	3 668	5 447
C(20)	5 255(4)	8 394(4)	1 278(3)	C(46)	9 205	2 718	5 349
C(21)	4 725(4)	6 276(4)	1 481(2)	C(52)	9 356(4)	2 476(3)	3 324(2)
C(22)	5 853(5)	7 784(5)	2 552(3)	C(53)	8 090(7)	3 446(5)	2 234(3)
C(23)	3 320(5)	6 012(4)	2 821(3)	C(54)	10 533(7)	4 215(5)	2 713(4)
C(24)	3 757(5)	8 104(4)	3 421(3)	C(55)	9 792(7)	2 247(5)	1 974(3)
C(25)	1 446(4)	7 134(4)	2 774(2)	C(56)	11 745(5)	2 038(6)	3 304(3)
C(26)	550(5)	9 200(3)	1 810(2)	C(57)	11 443(6)	3 557(6)	4 261(4)
C(27)	260(5)	9 670(4)	1 198(3)	C(58)	10 664(6)	1 406(6)	4 348(3)
C(28)	−342(6)	9 345(4)	2 222(3)	C(59)	5 598(5)	3 791(4)	3 054(3)
C(29)	1 724(5)	9 677(4)	2 151(3)	C(60)	5 531(7)	4 184(5)	2 409(3)
C(30)	−1 036(4)	6 873(3)	1 431(2)	C(61)	4 402(5)	3 414(5)	3 142(3)
C(31)	−911(5)	5 905(4)	1 132(3)	C(62)	6 107(6)	4 600(5)	3 561(4)
C(32)	−1 927(4)	7 296(4)	990(3)	C(63)	5 867(6)	1 420(4)	2 660(3)
C(33)	−1 446(5)	6 730(4)	2 052(3)	C(64)	5 112(7)	1 520(5)	2 032(3)
				C(65)	6 759(6)	863(4)	2 513(3)
				C(66)	5 116(6)	847(4)	3 078(3)
Compound **7**							
P	1 950(1)	130(1)	−113(1)	C(18)	2 196(1)	−1 859(1)	−1 176(2)
Si	3 251(1)	174(1)	−9(1)	C(19)	3 610(1)	−479(1)	−1 216(2)
C(1)	1 597(1)	63(1)	−1 805(2)	C(20)	3 350(1)	−389(1)	−2 487(2)
C(2)	1 441(1)	789(1)	−2 498(2)	C(21)	3 555(1)	−932(1)	−3 359(2)
C(3)	1 429(1)	752(1)	−3 786(2)	C(22)	4 031(1)	−1 573(1)	−2 982(2)
C(4)	1 491(1)	42(1)	−4 438(2)	C(23)	4 313(1)	−1 662(1)	−1 736(2)
C(5)	1 496(1)	−662(1)	−3 759(2)	C(24)	4 101(1)	−1 125(1)	−867(2)
C(6)	1 534(1)	−682(1)	−2 460(2)	C(25)	3 595(1)	1 235(1)	−125(2)
C(7)	1 197(1)	1 595(1)	−1 945(2)	C(26)	3 992(1)	1 484(1)	−1 088(2)
C(8)	1 843(1)	2 045(1)	−1 165(2)	C(27)	4 183(1)	2 291(2)	−1 216(2)
C(9)	544(1)	1 430(1)	−1 156(2)	C(28)	3 977(1)	2 858(1)	−394(2)
C(10)	861(1)	2 180(1)	−2 967(2)	C(29)	3 601(1)	2 623(1)	584(2)
C(11)	1 497(1)	65(1)	−5 853(2)	C(30)	3 419(1)	1 821(1)	723(2)
C(12)	2 207(1)	527(1)	−6 142(2)	C(31)	3 628(1)	−244(1)	1 563(2)
C(13)	1 518(1)	−776(1)	−6 414(2)	C(32)	4 289(1)	81(1)	2 225(2)
C(14)	778(1)	488(1)	−6 482(2)	C(33)	4 639(1)	−275(1)	3 308(2)
C(15)	1 445(1)	−1 520(1)	−1 852(2)	C(34)	4 334(1)	−960(1)	3 760(2)
C(16)	1 161(1)	−2 153(1)	−2 843(2)	C(35)	3 675(1)	−1 285(1)	3 143(2)
C(17)	825(1)	−1 484(1)	−978(2)	C(36)	3 330(1)	−930(1)	2 056(2)
Compound **10**							
P	7 681(1)	2 819(1)	3 439(1)	C(11)	7 609(3)	4 555(2)	5 503(2)
Si(1)	8 860(1)	3 144(1)	4 006(1)	C(12)	7 770(2)	4 034(2)	4 946(2)
Si(2)	8 009(1)	2 446(1)	2 317(1)	C(13)	9 468(2)	2 294(2)	4 406(2)
Si(3)	7 181(1)	1 733(1)	3 995(1)	C(14)	9 535(2)	2 207(2)	5 136(3)
C(1)	9 510(2)	3 724(2)	3 352(2)	C(15)	9 961(3)	1 582(2)	5 453(3)
C(2)	10 282(2)	3 474(2)	3 094(2)	C(16)	10 351(2)	1 022(2)	5 027(3)
C(3)	10 708(2)	3 894(2)	2 582(3)	C(17)	10 296(2)	1 094(2)	4 297(3)
C(4)	10 381(3)	4 593(2)	2 315(2)	C(18)	9 863(2)	1 719(2)	3 991(2)
C(5)	9 632(3)	4 865(2)	2 573(2)	C(19)	8 110(3)	3 378(3)	1 786(2)
C(6)	9 203(2)	4 432(2)	3 081(2)	C(20)	7 112(2)	1 854(3)	1 973(2)
C(7)	8 581(2)	3 839(2)	4 749(2)	C(21)	8 966(2)	1 846(2)	2 185(2)
C(8)	9 225(2)	4 202(2)	5 135(2)	C(22)	7 800(3)	813(2)	3 827(3)
C(9)	9 067(3)	4 717(2)	5 697(2)	C(23)	6 097(2)	1 586(2)	3 679(3)
C(10)	8 255(3)	4 889(2)	5 876(2)	C(24)	7 130(3)	1 957(3)	4 962(2)

unit, one of which is shown in Fig. 4. The co-ordination at the arsenic centres is quite pyramidal [Σ°As = 316° (av.)] with average interligand angles of 113.4, 102.7 and 99.8°. The widest angles involve the very bulky $SiPh_3$ and $CH(SiMe_3)_2$ groups. There is also a large angle 70.6° (av.) between the bisectors of the C–As–Si and C–Ga–C planes. The co-ordination at gallium is distorted trigonal planar with angles that span the range 113.8(2)–124.8(2)°. The Ga–As and Ga–C bonds are 2.459 (av.) and 2.019 Å (av.) in length. The As–C and As–Si distances are 2.025 (av.) and 2.366 Å (av.), respectively.

$(Ph_3Si)P(R)R'$ (R, R' = $C_6H_2Bu^t_3$-2,4,6, H **7**; $SiMe_3$, $SiMe_3$ **10**). The molecular structures of the asymmetrically substituted phosphine, **7**, and trisilylphosphine, **10** are illustrated in Figs. 5 and 6. In both molecules the co-ordination at the phosphorus centres is strongly pyramidal. The sum of angles, Σ°P, at phosphorus are 303.9° (**7**) and 321.3° (**10**). The P–Si bond lengths are P–Si 2.293(1) Å (**7**) and P–Si(1) 2.243(2) Å, P–Si(2) 2.261(2) Å and P–Si(3), 2.254(2) Å (**10**). In addition, the P–C and P–H distances for **7** are 1.863(2) and 1.199(22) Å, respectively.

Phosphorus-31 and Variable-temperature ^{1}H *NMR Studies.*—Table 6 presents the ^{31}P NMR chemical shifts for compounds **1–5**, **7–11** and other related species. The temperature dependence of the ^{1}H NMR spectra of **2–4** and **6–8** in the range +100 to −100 °C was investigated in C_7D_8 solution. A similar study of **1**, as previously communicated,[6] indicated a splitting of the $GaBu^t_2$ singlet at low temperatures (see Fig. 7). A barrier of 12.7 kcal mol^{-1} was estimated for the dynamic process. Energy barriers ($\Delta G^{\ddagger}$) for the observed dynamic processes were

Table 4 Selected bond distances (Å) and angles (°) for compounds Bu^t_2GaPRR' **1**, **2** and **12**[a]

	1	2	12
Ga–P	2.295(3)	2.296(1)	2.319(1)
P–R[a]	2.259(4)	2.249(2)	1.838(3)
P–R'[a]	1.890(8)	1.847(3)	1.820(3)
Ga–C	2.014(11)	2.008(4)	2.012(3)
	2.015(11)	2.016(4)	2.005(3)
R–P–R'	108.6(3)	104.6(1)	116.0(1)
Ga–P–R	125.3(1)	128.9(1)	117.3(1)
Ga–P–R'	112.5(3)	107.0(1)	110.9(1)
C–Ga–C	119.1(4)	122.0(1)	126.7(1)
C–Ga–P	121.2(3)	119.3(1)	116.6(1)
	112.5(3)	117.2(1)	115.8(1)
Sum of angles at phosphorus (Σ°P)	346.4	340.5	344.2
Twist angle[b]	3.9	1.9	56.4

[a] R,R' = $SiPh_3$, $C_6H_2Bu^t_3$-2,4,6 **1**; $SiPh_3$, $C_6H_2Pr^i_3$-2,4,6 **2**; $B(C_6H_2Me_3$-2,4,6$)_2$, Ph **12**. [b] Defined as the angles between the perpendiculars to the R–P–R' and C–Ga–C planes when viewed along the Ga–P bonds.

Table 5 Selected bond distances (Å) and angles (°) for compounds **5**–**7** and **10**

Compound **5**

P–Al	2.416(3)	Si–P–Al	126.9(1)
P–Si	2.223(3)	Si–P–C(1)	105.3(2)
Si–C(16)	1.887(6)	Al–P–C(1)	119.4(2)
Si–C(22)	1.894(6)	P–Al–O	101.0(2)
Si–C(28)	1.869(7)	P–Al–C(34)	116.4(2)
Al–O	1.950(6)	P–Al–C(38)	109.0(2)
Al–C(34)	2.017(6)	C(34)–Al–C(38)	116.3(3)
Al–C(38)	2.025(6)	O–Al–C(34)	109.2(3)
		O–Al–C(38)	102.9(2)

Compound **6**

As(1)–Ga(1)	2.458(1)	Si(4)–C(46)	1.906(3)
As(1)–Si(1)	2.371(1)	Si(5)–C(52)	1.892(5)
As(1)–C(19)	2.022(4)	Si(6)–C(52)	1.906(5)
Ga(1)–C(26)	2.019(5)		
Ga(1)–C(30)	2.019(4)	Ga(1)–As(1)–Si(1)	100.9(1)
Si(1)–C(1)	1.920(4)	Ga(1)–As(1)–C(19)	102.7(1)
Si(1)–C(7)	1.891(3)	Si(1)–As(1)–C(19)	113.7(1)
Si(1)–C(13)	1.916(3)	As(1)–Ga(1)–C(26)	124.8(2)
Si(2)–C(19)	1.870(5)	As(1)–Ga(1)–C(30)	113.8(2)
Si(3)–C(19)	1.907(5)	C(26)–Ga(1)–C(30)	121.4(2)
As(2)–Ga(2)	2.461(1)	Ga(2)–As(2)–Si(4)	98.8(1)
As(2)–Si(4)	2.362(2)	Ga(2)–As(2)–C(52)	102.7(1)
As(2)–C(52)	2.028(5)	Si(4)–As(2)–C(52)	113.2(1)
Ga(2)–C(59)	2.012(6)	As(2)–Ga(2)–C(59)	114.7(1)
Ga(2)–C(63)	2.026(5)	As(2)–Ga(2)–C(63)	124.7(2)
Si(4)–C(34)	1.910(4)	C(59)–Ga(2)–C(63)	120.6(2)
Si(4)–C(40)	1.897(3)		

Compound **7**

P–Si	2.293(1)	Si–P–C(1)	104.9(1)
P–C(1)	1.863(2)	Si–P–H	93(1)
P–H	1.199(22)	C(1)–P–H	106(1)
Si–C(19)	1.874(2)	P–Si–C(19)	112.1(1)
Si–C(25)	1.876(2)	P–Si–C(25)	111.1(1)
Si–C(31)	1.881(2)	P–Si–C(31)	105.6(1)

Compound **10**

P–Si(1)	2.243(2)	Si(1)–P–Si(2)	108.2(1)
P–Si(2)	2.261(2)	Si(1)–P–Si(3)	106.3(1)
P–Si(3)	2.254(2)	Si(2)–P–Si(3)	106.8(1)
Si(1)–C(1)	1.887(4)	P–Si(1)–C(1)	106.6(1)
Si(1)–C(7)	1.876(4)	P–Si(1)–C(7)	107.7(1)
Si(1)–C(13)	1.890(4)	P–Si(1)–C(13)	116.2(1)

calculated by using an approximate formula as previously described.[21] For **2**, overlap of the *o*-$CH(CH_3)_2$ and $GaBu^t_2$ resonances in the above temperature range prevented a useful

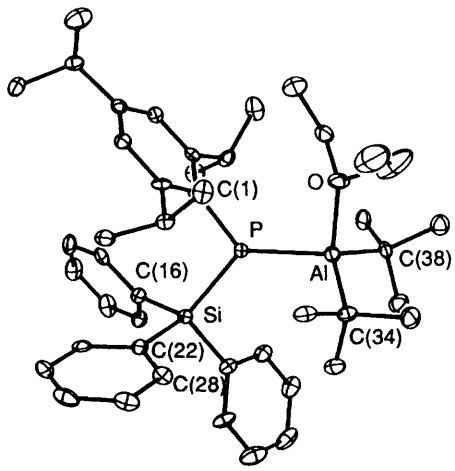

Fig. 3 Computer-generated thermal ellipsoid (30%) plot of compound **5**. Hydrogen atoms are omitted for clarity

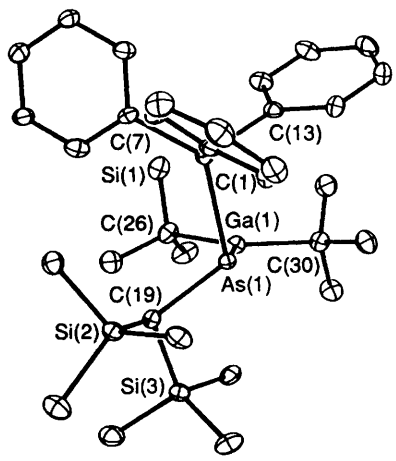

Fig. 4 Computer-generated thermal ellipsoid (30%) plot of compound **6**. Hydrogen atoms are omitted for clarity

interpretation of the dynamic behaviour. For the species **3**, **4** and **6** all signals were well separated and splitting of the $GaBu^t_2$ singlet was not observed at temperatures as low as −100 °C. In fact no dynamic behaviour involving the other resonances in the species **3**, **4** and **6** was observed. In the case of **7**, at 25 °C, broad and sharp *o*-Bu^t and *p*-Bu^t singlets, respectively, were observed. Cooling the sample resulted in splitting of the *o*-Bu^t peak into two signals. Taking a T_c of 15 °C and a maximum peak separation of 57 Hz at −80 °C gives a barrier of 14.1 kcal mol^{-1} for this dynamic process. For the $C_6H_2Pr^i_3$-2,4,6 analogue **8**, two well resolved sets of doublets were observed for the *o*-$CH(CH_3)_2$ protons at 25 °C. Upon increasing the temperature, the doublets broadened and coalescence of both sets of peaks was observed at T_c = 75 °C (Fig. 8). This T_c, along with a maximum peak separation of 83.4 Hz at 25 °C, gives a barrier ($\Delta G^{\ddagger}$) of *ca.* 16.9 kcal mol^{-1} for the dynamic process. Decreasing the temperature resulted in broadening of both *o*-$CH(CH_3)_2$ and *o*-$CH(CH_3)_2$ resonances. The *o*-$CH(CH_3)_2$ doublets appear to merge into a broad singlet and below −70 °C resolve into two or more broad singlets. In the case of the *o*-$CH(CH_3)_2$ septet, splitting into two broad peaks at T_c = −65 °C was observed becoming sharper as the temperature is decreased. Taking this T_c and a peak separation of 243 Hz at −90 °C gives a $\Delta G^{\ddagger}$ of 9.43 kcal mol^{-1}. Singlets were observed for the mesityl *o*- and *p*-Me and *m*-H hydrogens of $(Ph_3Si)P(C_6H_2Me_3$-2,4,6)H **9** at ambient temperature. Cooling of **9** in [$^2H_8$]toluene caused a splitting of both the *o*-Me and *m*-H resonances. The approximate coalescence temperatures and peak separations (at −98 °C) of −80 °C and 104 Hz (*o*-Me)

Table 6 Phosphorus-31 NMR chemical shift values for **1–5**, **7–11** and other related compounds

Compound	$\delta(^{31}P)^a$
1 $Bu^t_2GaP(C_6H_4Bu^t_3\text{-}2,4,6)(SiPh_3)$	−119
2 $Bu^t_2GaP(C_6H_2Pr^i_3\text{-}2,4,6)(SiPh_3)$	−146
3 $Bu^t_2GaP(C_6H_2Me_3\text{-}2,4,6)(SiPh_3)^b$	−141
4 $Bu^t_2GaP(SiMe_3)(SiPh_3)$	−267
5 $Bu^t_2Al(Et_2O)P(C_6H_2Pr^i_3\text{-}2,4,6)(SiPh_3)$	−199
7 $(Ph_3Si)P(C_6H_2Bu^t_3\text{-}2,4,6)H$	−132 ($^1J_{PH}$ 220 Hz)
8 $(Ph_3Si)P(C_6H_2Pr^i_3\text{-}2,4,6)H$	−169 ($^1J_{PH}$ 211 Hz)
9 $(Ph_3Si)P(C_6H_2Me_3\text{-}2,4,6)H$	−162 ($^1J_{PH}$ 210 Hz)
10 $(Ph_3Si)P(SiMe_3)_2$	−254
11 $(Me_3Si)(Ph_3Si)PLi\cdot dme^b$	−315
$Bu^tGa[PH(C_6H_2Bu^t_3\text{-}2,4,6)_2]$	−113 ($^1J_{PH}$ 203 Hz)[22]
$Ga[PH(C_6H_2Bu^t_3\text{-}2,4,6)_2]_3$	−91.6 ($^1J_{PH}$ 216 Hz)[22]

[a] Referenced externally to 85% H_3PO_4; in C_6D_6 unless otherwise stated. [b] In C_7D_8.

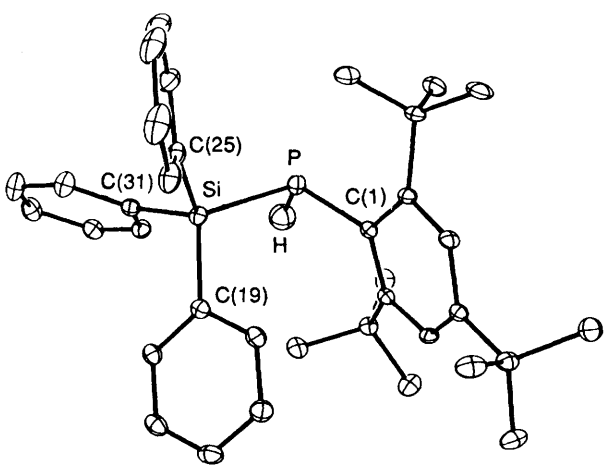

Fig. 5 Computer-generated thermal ellipsoid (30%) plot of compound **7**. Hydrogen atoms except for the phosphorus hydrogen are omitted for clarity

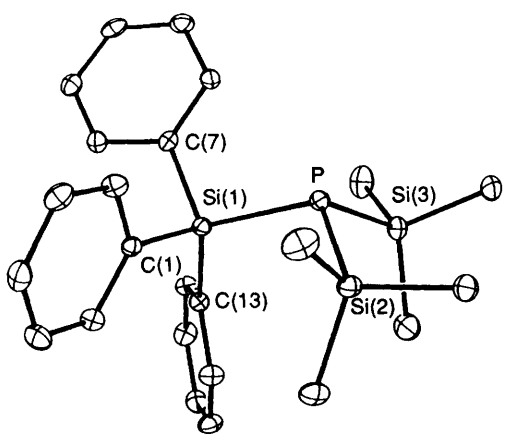

Fig. 6 Computer-generated thermal ellipsoid (30%) plot of compound **10**. Hydrogen atoms are omitted for clarity

and −90 °C and 47.1 Hz (*m*-H) afforded similar barriers of 9.05 and 8.85 kcal mol^{-1}, respectively.

Discussion

Syntheses.—The high yield syntheses of the bulky arylsilylphosphines **7–9** was accomplished in Et_2O solution by a salt-elimination reaction between the primary phosphide LiPHR (R = $C_6H_2Bu^t_3$-2,4,6, $C_6H_2Pr^i_3$-2,4,6 or $C_6H_2Me_3$-2,4,6) and

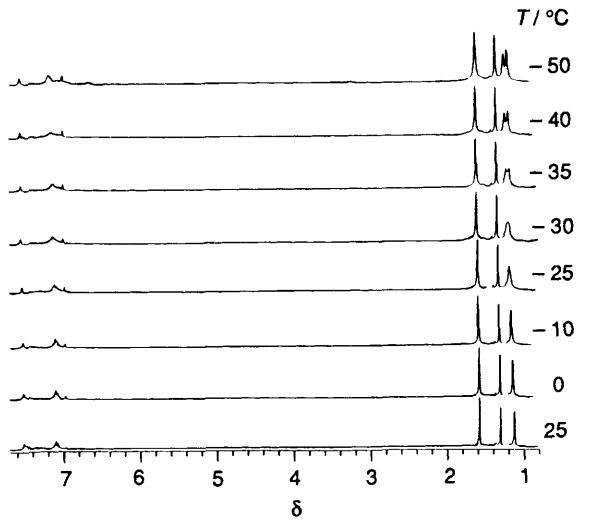

Fig. 7 Variable-temperature ^1H NMR study (−50 to +25 °C) of $Bu^t_2GaP(C_6H_2Bu^t_3\text{-}2,4,6)(SiPh_3)$ **1**

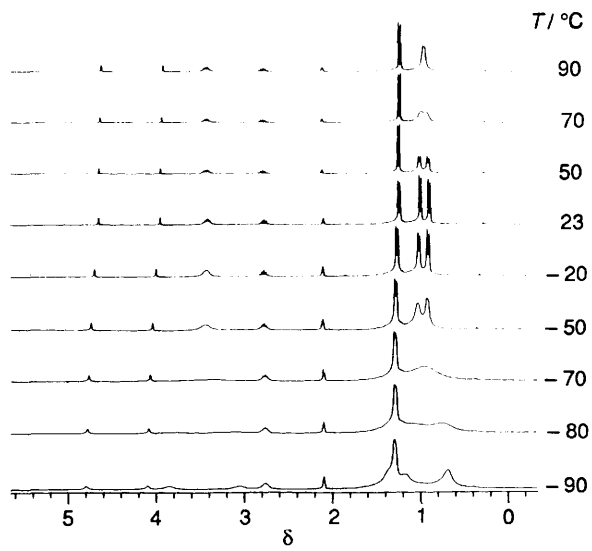

Fig. 8 Variable-temperature ^1H NMR study (−90 to +90 °C) of $(Ph_3Si)P(C_6H_2Pr^i_3\text{-}2,4,6)H$ **8**

Ph_3SiCl. A similar method was used to synthesize the asymmetric arsine $(Ph_3Si)As[CH(SiMe_3)_2]H$ used in the preparation of the monomeric arsinogallane **6**. The synthetic route to the disilylphosphide $(Me_3Si)(Ph_3Si)PLi\cdot dme$ **11**, was not as straightforward as illustrated by equations (1) and (2).

$$(Me_3Si)_2PLi\cdot 2thf + Ph_3SiCl \xrightarrow[0\ °C]{Et_2O,\ -LiCl} (Ph_3Si)P(SiMe_3)_2 \quad (1)$$

$$(Ph_3Si)P(SiMe_3)_2 + LiMe \xrightarrow[-10\ °C]{dme,\ -SiMe_4} (Me_3Si)(Ph_3Si)PLi\cdot dme \quad (2)$$

The first step involved treatment of $(Me_3Si)_2PLi\cdot 2thb$ with Ph_3SiCl to give $(Ph_3Si)P(SiMe_3)_2$ **10** [equation (1)] followed by the addition of methyllithium to **10** in dme to yield the asymmetric lithium salt of **10** [equation (2)]. The phosphinogallanes **1–4**, and arsenogallane **6**, and the aluminium phosphide **5** were also prepared by salt-elimination reaction as shown in equation (3), where M = Ga or Al, E = P or As, R = bulky aryl, alkyl or silyl group. In the case of **5** (M = Al,

$$MBu^t_2Cl + Li(Ph_3Si)E(R) \xrightarrow[0\ ^\circ C]{Et_2O,\ -LiCl} Bu^t_2ME(R)(SiPh_3) \quad (3)$$

E = P), the greater Lewis acidity of Al as compared to Ga results in a stable Et_2O adduct.

Structures.—The series of compounds **1–3** represent the first well characterized examples of unassociated monophosphinogallanes. In these compounds any possible π interaction between the gallium and phosphorus is confined to one bond. Thus these simple molecular Ga–P species allow the strength of the Ga–P π interaction to be more easily assessed. Structural and spectroscopic evidence for moderately strong π bonding in boron–nitrogen and –phosphorus $R_2BE(R')R''$ (E = N and P) analogues of **1–3** has been previously observed.[1,2,9] Manifestations of π bonding include B–E bond shortening and low angles between the lone pair on nitrogen or phosphorus and the empty 2p orbital on boron. In addition, barriers to rotation around the B–E bonds as high as 25 kcal mol^{-1} have been reported.[9,22]

Perhaps the most interesting aspect of the data in Table 4 is the correlation between Ga–P bond length and twist angle between the lone pair of phosphorus and the empty p orbital of gallium. For example, when the twist angles are less than 4°, as in **1** and **2**, the Ga–P bonds are 2.295(1) and 2.296(1) Å. This trend also extends to the partially refined structure of **4** in which the Ga–P bond length is 2.358(4) Å and the twist angle is 76.5°. It is also noteworthy that in spite of the large substituents in **1** and **2** the Ga–P distances are at the lower end of the currently known range for Ga–P single bonds.*[23] If the Ga–P bond were purely of a σ type, steric interactions could have been reduced by a rotation of the gallium and phosphorus ligand sets with respect to each other. It is therefore probable that there is a weak π interaction in the Ga–P bond. An analysis of various other structural details of **1**, **2** and **4** supports this view. The change in the Ga–P distance between **1**, **2** (both *ca.* 2.295 Å) and the partially refined **4** [2.358(4) Å] may be due either to the presence of a Ga–P π bond or a change in hybridization at phosphorus or both. Unfortunately, the relatively small (0.063 Å) range of the Ga–P distances in **1**, **2** and **4** makes the distinction between the effects of σ and π bonding difficult to assess. It is notable, however, that the difference between P–Si distances in **1** [2.259(4) Å] and that in its precursor **7** [2.293(1) Å] is 0.034 Å. The P–C distance in **1** [1.890(8) Å] is actually longer (presumably for steric reasons) than that observed in **7** [1.863(2) Å]. It appears, therefore, that as a result of σ-bonding changes a shortening of only 0.034 Å is expected in the Ga–P bond in this system. The actual difference observed between the Ga–P bonds in **1** and **4** is 0.063 Å. In addition, if it is borne in mind that the ligand set ($C_6H_2Bu^t_3$-2,4,6 and $SiPh_3$) on phosphorus in **1** is also more crowding than that ($SiMe_3$ and $SiPh_3$) in **4**, it seems reasonable to conclude that the bond distances observed in **1** are indicative of weak π bonding. The weakness of this π interaction is apparent from a comparison with the structure $Bu^t_2GaP(Ph)B(C_6H_2Me_3$-2,4,6$)_2$ **12**.[20] In this compound competition exists between the empty boron and gallium p orbitals for a share of the single phosphorus lone pair. In **12**, the Ga–P distance is 2.319(1) Å and the angle between the planes at gallium and phosphorus is 56.4°. These values lie between those of **1**, **2** and **4**. In contrast, the B–P bond, 1.838(3) Å in **12** is relatively short and the angle between the boron–phosphorus p orbitals is less than 10°. In other words, the π bonding in **12** is dominated by a B–P rather than a Ga–P interaction.

The structures of the bulky phosphines $(Ph_3Si)P(C_6H_2Bu^t_3$-2,4,6$)H$ **7** and $(Ph_3Si)P(SiMe_3)_2$ **10** were determined to investigate bond lengths (*i.e.* P–Si and P–C) and geometry around the phosphorus centres in the absence of the $GaBu^t_2$ ligand. To our knowledge, **10** represents the first X-ray crystal structure of a trisilylphosphine. The sum of angles around the phosphorus atoms in both **7** and **10**, 303.9 and 321.3°, indicate strongly pyramidal co-ordination at phosphorus. In the case of the trisilyl species **10**, a more planar phosphorus co-ordination might have been expected since it is well known that silyl substituents reduce the inversion barrier at phosphorus by *ca.* 42, 37 and 25% for each successive substitution.[8] The sum of angles at phosphorus for **7** lies below, and those of **10** between, those in the structures of PPh_3 ($\Sigma°P = 310°$)[24] and $P(C_6H_2Me_3$-2,4,6$)_3$ ($\Sigma°P = 329°$).[25] A comparison of the structures of **4** and **10** supports the conclusions drawn from the discussion of the structures of **1** and **7** in the preceding paragraph. In the case of **4** and **10**, the pyramidicities at the phosphorus atoms differ only slightly (326.2 *vs.* 321.3°) and only small differences (0.02 Å) are observed in the P–Si distances. Presumably, the similar size of the $SiMe_3$ and $GaBu^t_2$ ligands along with the absence of a Ga–P π interaction in **4** account for the structural similarity.

The compound $Bu^t_2Al(Et_2O)P(C_6H_2Pr^i_3$-2,4,6$)(SiPh_3)$ **5** was obtained during attempts to synthesize aluminium–phosphorus analogues of **1–4**. These species, successfully prepared, would also have represented a new class of Al–P compounds. The structure of **5**, in contrast to those of **1–4**, contains an Et_2O molecule bound to the aluminium centre. This result is in harmony with the greater size and higher Lewis acidity of aluminium in comparison to gallium. The molecule of **5**, however, has some interesting features. One is that the geometry at phosphorus is almost flat and approaches planarity ($\Sigma°P = 351.6°$). Presumably, this is a consequence of steric crowding and the electropositive nature of aluminium and the silyl substituents. Furthermore, the Al–P bond length, 2.416(3) Å, although ≈0.06 Å shorter than that seen in the dimeric species $(Ph_2PAlBu^i_2)_2$ [2.476(1) Å],[26] is comparable to Al–P in the cubane, $[Bu^tAl(\mu_3\text{-}PSiPh_3)]_4$ [2.414 Å (av.)].[27] The Al–O bond [1.950(6) Å] in **5** is slightly longer than those of other ether adducts of aluminium, $(PhH_2C)_3Al{\cdot}OEt_2$ [1.901(4) Å][28] and $(C_6H_4Me\text{-}o)_3Al{\cdot}OEt_2$ [1.928(3) Å].[29] Presumably, this lengthening is also a consequence of the greater crowding at aluminium in **5**.

The structure of **6** was determined to allow direct structural comparisons between phosphorus and arsenic in compounds of similar formulae to **1–4**. Attempts to make a phosphorus analogue of **6** have proved unsuccessful so far. Well characterized monomeric arsinogallanes in the species $Bu^t_2GaAsBu^t_2$ **13** [Ga–As 2.466(3) Å, $\Sigma°As \approx 317°$][30] and $(C_5Me_5)_2GaAs(SiMe_3)_2$ **14** [Ga–As 2.433(4) Å, $\Sigma°As \approx 320°$][31] have already appeared in the literature. Compound **6**, however, is the first structurally characterized monomeric arsinogallane in which arsenic is asymmetrically substituted. This permits measurement of restricted rotation around the Ga–As bond by variable-temperature ^1H NMR methods (see below). The structure of **6**, however, is similar to those previously reported. The Ga–As single bond distance of 2.459 Å (av.) is comparable with the sum of covalent radii of Ga and As.[32,*] As for **13** and **14**, the co-ordination at arsenic is strongly pyramidal [$\Sigma°As = 316°$ (av.)] and the twist angle between the lone pair of arsenic and the empty p orbital of Ga is high, 70.6° (av.). These structural parameters suggest that the Ga–As bond is a simple σ bond with no π component.

NMR Studies.—A common feature of all Ga–P compounds listed in Table 6 is their upfield ^{31}P chemical shift. This is in sharp contrast to their boron–phosphorus analogues which have positive δ values. The more negative δ values of the gallium derivatives may be attributed to higher electron density on the phosphorus centre owing to the presence of the electropositive silyl and gallyl substituents. The weakness of Ga–P π bonding suggests that the phosphorus lone pair electron density remains

* For example Ga–P = 2.34(1) Å in $Ga[PH(C_6H_2Bu^t_3$-2,4,6$)]_3$ and 2.32 Å in $Bu^tGa[PH(C_6H_2Bu^t_3$-2,4,6$)]_2$.

located on phosphorus. Presumably, this also contributes to the upfield chemical shift. The large negative δ values observed for **4**, **10** and **11** are due to the increased number of electropositive ligands (i.e. SiR_3, $GaBu^t_2$ or Li^+) at phosphorus. Two opposing factors account for the intermediate ^{31}P shift of **5**; removal of electron density at phosphorus by rehybridization of the lone pair orbital from s to p character and electron donation to phosphorus through the Al–P σ bond. As expected, species with more planar phosphorus co-ordination in the series **1–3** and corresponding ligands **7–9** have the most downfield ^{31}P chemical shifts. The J_{PH} coupling constants of **7–9** also support this correlation. A larger J_{PH} (**7**) corresponds to greater s character in the phosphorus bonding orbital to hydrogen. The shifts and coupling constants of **2** and **3**, and **8** and **9** suggest similar environments at the phosphorus centres.

A variable-temperature ^1H NMR study was undertaken to investigate the strength of possible Ga–P multiple bonding in **2–4**. A similar study of **1** was reported in a preliminary communication.[6] In this case a barrier of 12.7 kcal mol^{-1} to rotation around the Ga–P bond was observed. The variable-temperature ^1H NMR study of **2** was inconclusive owing to peak overlap, and splitting of the $GaBu^t_2$ singlet for **3** and **4** was not observed at temperatures as low as −100 °C. Therefore, the upper limit on Ga–P π bonding in **3** and **4** (taking a T_c of −100 °C) is probably not greater than 8–9 kcal mol^{-1}. In the case of **4**, this data is consistent with structural evidence which suggests insignificant Ga–P p–p π overlap. It is also compatible with the structural differences observed in **1** and the larger barrier (12.7 kcal mol^{-1}) to rotation around the Ga–P bond. The variable-temperature ^1H NMR studies of the precursor phosphines **7–9** were undertaken to assess barriers to inversion of these new and sterically bulky asymmetric phosphines. Typically, inversion barriers have been measured by observing the temperature dependence of magnetically inequivalent diastereotopic groups such as the methyls of a prochiral ligand [*i.e.* $R(R')PCHMe_2$].† These groups become enantiotopic when inversion is fast on the NMR time-scale and coalescence is usually observed. In the compounds **7–9** $(Ph_3Si)P(C_6H_2R_3$-2,4,6)H (R = Bu^t **7**, Pr^i **8** or Me **9**) the *o*-R groups have in effect the same function as the diastereotopic groups described above and may exhibit magnetic inequivalence even in the presence of fast P–C(aryl) bond rotation. The ^1H NMR data for **8** indicate the presence of two temperature-dependent processes that have barriers of *ca.* 9.43 and 16.9 kcal mol^{-1}. These two processes may be assigned to either inversion barrier at phosphorus or to aromatic ring flip. The latter is also a possibility since variable-temperature ^1H NMR studies of arylboryloxides such as $B(OMe)(C_6H_2Me_3$-2,4,6)$_2$ have given barriers as high as 12 kcal mol^{-1} which were assigned to ring flip of the mesityl groups.[35] We note, however, that inversion barriers for the monosilylphosphines $PhP(SiMe_3)CHMe_2$ and Ph(Me)P-$(SiPhMe_2)$ are *ca.* 19 kcal mol^{-1}.[36] This value is more consistent with the larger barrier detected for **8**. Moreover, the larger value observed for **7** (14.2 kcal mol^{-1}), is in harmony with this result because of the greater steric crowding in **7**. The barrier observed in the case of **9** is very similar to that in **8**.

* The radius of gallium is difficult to estimate owing to the complicated structure of the element itself.[33]

† For theoretical discussions and/or inversion barrier determinations at Group 15 elements see ref. 34.

Acknowledgements

We thank the National Science Foundation for financial support.

References

1 K. Niedenzu and J. W. Dawson, *Boron-Nitrogen Compounds*, Springer-Verlag, Berlin, 1964.
2 M. F. Lappert, P. P. Power, A. R. Sanger and R. C. Srivastava, *Metal and Metalloid Amides*, Ellis-Horwood, Chichester, 1979.
3 P. P. Power, *Angew. Chem., Int. Ed. Engl.*, 1990, **29**, 449.
4 M. A. Petrie, S. C. Shoner, H. V. R. Dias and P. P. Power, *Angew. Chem., Int. Ed. Engl.*, 1990, **29**, 1033.
5 H.-G. von Schnering, M. Somer, M. Hartweg and K. Peters, *Angew. Chem., Int. Ed. Engl.*, 1990, **29**, 65.
6 M. A. Petrie, K. Ruhlandt-Senge and P. P. Power, *Inorg. Chem.*, 1992, **31**, 4038.
7 M. A. Petrie and P. P. Power, *Inorg. Chem.*, 1993, **32**, 1309.
8 K. Mislow, *Trans. N. Y. Acad. Sci.*, 1973, **35(3)**, 227.
9 D. C. Pestana and P. P. Power, *J. Am. Chem. Soc.*, 1991, **113**, 8426.
10 W. M. Cleaver and A. R. Barron, *Chemtronics*, 1989, **4**, 146.
11 W. Uhl, J. Wagner, D. Fenske and G. Baum, *Z. Anorg. Allg. Chem.*, 1992, **612**, 25.
12 A. H. Cowley, N. C. Norman and M. Pakulski, *Inorg. Synth.*, 1990, **27**, 237.
13 Y. van den Winkel, H. M. M. Bastiaans and F. Bickelhaupt, *J. Organomet. Chem.*, 1991, **405**, 183.
14 T. Oshikawa and M. Yamashita, *Chem. Ind.*, 1985, 126.
15 G. Fritz and W. Holderich, *Z. Anorg. Allg. Chem.*, 1977, **422**, 104.
16 R. L. Wells, K. Chong-Yon, A. P. Purdy, A. T. McPhail and C. G. Pitt, *Polyhedron*, 1990, **9**, 319.
17 See, H. Hope, *Experimental Organometallic Chemistry: A Practicum in Synthesis and Characterization*, eds. A. L. Wayda and M. Y. Darensbourg, ACS Symp. Ser. 357, American Chemical Society, Washington D.C., 1987, ch. 10.
18 G. M. Sheldrick, SHELXTL PLUS, Program for Crystal Structure Determinations, University of Göttingen, 1986.
19 *International Tables for X-Ray Crystallography*, Kynoch Press, Birmingham, 1974, vol. 4.
20 J. J. Ellison, K. Ruhlandt-Senge and P. P. Power, unpublished work.
21 D. Kost, E. H. Carlson and M. J. Raban, *J. Chem. Soc., Chem. Commun.*, 1971, 656.
22 R. H. Neilson and R. L. Wells, *Inorg. Chem.*, 1977, **16**, 7.
23 A. M. Arif, B. L. Benac, A. H. Cowley, R. Geerts, R. A. Jones, K. B. Kidd, J. M. Power and S. T. Schwab, *J. Chem. Soc., Chem. Commun.*, 1986, 1543; D. A. Atwood, A. H. Cowley, R. A. Jones and M. A. Mardones, *J. Am. Chem. Soc.*, 1991, **113**, 7051.
24 J. J. Daly and S. A. Zuerick, *Z. Kristallogr.*, 1963, **118**, 322.
25 J. F. Blount, C. A. Maryanoff and K. Mislow, *Tetrahedron Lett.*, 1975, **11**, 913.
26 S. A. Sangokoya, W. T. Pennington and G. H. Robinson, *J. Organomet. Chem.*, 1990, **385**, 23.
27 A. H. Cowley, R. A. Jones, M. A. Mardones, J. L. Atwood and S. G. Bott, *Angew. Chem., Int. Ed. Engl.*, 1990, **29**, 1409.
28 A. F. M. Maqsudur Rahman, K. F. Siddiqui and J. P. Oliver, *J. Organomet. Chem.*, 1987, **319**, 161.
29 M. Barber, D. Liptak and J. P. Oliver, *Organometallics*, 1982, **1**, 1307.
30 K. T. Higa and C. George, *Organometallics*, 1990, **9**, 275.
31 E. K. Byrne, L. Parkanyi and K. H. Theopold, *Science*, 1988, **241**, 332.
32 J. E. Huheey, *Inorganic Chemistry*, Harper and Row, New York, 3rd edn., 1983, p. 258.
33 R. Nesper, *Angew. Chem., Int. Ed. Engl.*, 1991, **30**, 789.
34 W. D. Jennings, *Chem. Rev.*, 1975, **75**, 307; W. Egan and K. Mislow, *J. Am. Chem. Soc.*, 1971, **93**, 1805; A. Rauk, L. C. Allen and K. Mislow, *Angew. Chem., Int. Ed. Engl.*, 1970, **9**, 400.
35 P. Finocchiaro, D. Gust and K. Mislow, *J. Am. Chem. Soc.*, 1973, **95**, 7029; J. F. Blount, P. Finocchiaro, D. Gust and K. Mislow, *J. Am. Chem. Soc.*, 1973, **95**, 7019.
36 R. D. Baechler and K. Mislow, *J. Am. Chem. Soc.*, 1970, **92**, 4758.

Received 6*th November* 1992; *Paper* 2/05925H